

Capacity Evaluation of an Indoor Wireless Channel at 60 GHz Utilizing Uniform Rectangular Arrays

NEKTARIOS MORAITIS¹, DIMITRIOS DRES¹, ODYSSEAS PYROVOLAKIS²
¹National Technical University of Athens, Mobile Radiocommunications Laboratory
9 Heron Polytechniou, 15773, Zografou, Athens, Greece
Email: morai@mobile.ntua.gr, jdres@mobile.ntua.gr
²Hellenic Naval Academy
Terma Chatzikyriakou, 18537, Pireaus, Greece
Email: ody@telecom.ntua.gr

Abstract: - This paper studies the capacity of an indoor wireless system operating at 60 GHz using a physical channel model that incorporates multiple elements at both antenna terminals. The proposed channel model utilizes the geometric characteristics of the environment, the angle of arrival and angle of departure of each one of the propagation paths, the antenna elements and their spacing. The results showed that the system capacity increases significantly if SIMO, MISO or MIMO configuration is utilized instead of the basic SISO channel. The capacity decreases, as the distance between the terminals increase. In the 90% of the cases the capacity remains above 4 b/s/Hz, even when the receiver is 15 m away from the base station. Finally, very high data rates, even higher than 155 Mb/s, can be achieved maintaining low SNR.

Key-Words: - Capacity, millimeter wave propagation, multiple element antennas, wireless broadband systems.

1 Introduction

Over the last years, the force for broadband systems and in particular for mobile broadband communications to deal with new services requires high capacity. The demand for data rates greater than 2 Mb/s, up to 155Mb/s, is enormous and Wireless Broadband Systems (WBSs) are emerging rapidly. Such systems though cannot operate in the lower portions of spectrum, since large bandwidths are required. Therefore, the millimeter wave band and especially 60 GHz are promising [1], allocating a massive amount of spectral space (5 GHz). Using the 60 GHz band in combination with multiple element antennas at the terminals is expected to achieve explicit transmission rates (greater than 155 Mb/s) in order to provide enhanced broadband services.

MISO (Multiple Input Single Output) or SIMO (Single Input Multiple Output) systems have already been evaluated for the optimization of the system performance. Highest link capacity is expected if multiple antennas are used at both the receiver and the transmitter site - the so called MIMO systems (Multiple Input Multiple Output) - where have been theoretically investigated with rather impressive results, especially in terms of remarkable data rate improvements. In millimeter wave frequencies the propagation modeling, apart from the known

empirical models, can be realized based on geometrical optics using ray-tracing theory. In the 60 GHz region the diffraction phenomenon can be neglected, and the sum of the direct ray and the reflected rays is enough to describe the behavior of the propagation channel with great accuracy.

In this paper we evaluate the capacity of a multiple element antenna system at 60 GHz in indoor environments. In order to calculate the channel matrix that is required to assess the channel capacity, a physical channel model is used. The signal propagation at 60 GHz in an indoor environment is described with the help of geometrical optics so as to evaluate the capacity of the proposed system. The studied configuration utilizes Uniform Rectangular Arrays (URAs), which is used for 2-D (azimuth/elevation) resolution.

The remainder of this paper is organized as follows. Section 2 deals with the channel modeling and the proposed multi-ray model. In Section 3 an analytically description of the geometry of the environment under consideration is presented along with the simulation procedure of the proposed channel model, dealing with two different geometry scenarios. In Section 4, the results of the space-time channel model are presented taking into consideration the accomplishment of the capacity improvement ($C > 1$ b/s/Hz), in order to evaluate the

total throughput of the MIMO system. Finally, Section 5 is devoted to discussion and conclusions derived by the entire simulation procedure.

2 Channel Model

In order to calculate the capacity of a system with one antenna element at both terminals, the channel impulse response, $h(\tau)$, between the

$$\mathbf{a}_r(\phi, \theta) = \begin{bmatrix} 1 & e^{-j\frac{2\pi}{\lambda}\Delta l_r \cos(\phi)\cos(\theta)} & \dots & e^{-j\frac{2\pi}{\lambda}\Delta l_r (N_r-1)\cos(\phi)\cos(\theta)} \end{bmatrix}^T \quad (1\alpha)$$

$$\mathbf{a}_c(\theta) = \begin{bmatrix} 1 & e^{-j\frac{2\pi}{\lambda}\Delta l_c \sin(\theta)} & \dots & e^{-j\frac{2\pi}{\lambda}\Delta l_c (M_c-1)\sin(\theta)} \end{bmatrix}^T \quad (1\beta)$$

$$\mathbf{H} = \left[\text{vec}(\mathbf{A}(\phi_{R,1}, \theta_{R,1})) \quad \dots \quad \text{vec}(\mathbf{A}(\phi_{R,L}, \theta_{R,L})) \right] \begin{bmatrix} \beta_1 & 0 & 0 \\ 0 & \ddots & 0 \\ 0 & 0 & \beta_L \end{bmatrix} \left[\text{vec}(\mathbf{A}(\phi_{T,1}, \theta_{T,1})) \quad \dots \quad \text{vec}(\mathbf{A}(\phi_{T,L}, \theta_{T,L})) \right]^H \quad (3)$$

$$\underbrace{\beta_1 = \frac{1}{d_0}}_{\text{direct}}, \quad \underbrace{\beta_{2-5} = \sum_{i=1}^4 \frac{R_i}{d_i} e^{j\Delta\phi_i}}_{\text{single reflected}}, \quad \underbrace{\beta_{6-9} = \sum_{j=1}^4 \frac{R_{ja}R_{jb}}{d_j} e^{j\Delta\phi_j}}_{\text{double reflected}}, \quad \underbrace{\beta_{10-13} = \sum_{k=1}^4 \frac{R_{ka}R_{kb}R_{kc}}{d_k} e^{j\Delta\phi_k}}_{\text{triple reflected}} \quad (4)$$

The steering vectors combine to the steering matrix:

$$\mathbf{A}(\phi, \theta) = \mathbf{a}_c(\theta) \cdot \mathbf{a}_r(\phi, \theta)^T \quad (2)$$

where Δl_r and Δl_c are row/column spacing between the elements, N_r and M_c are the number of row/column elements respectively in either transmitter or receiver terminal, ϕ and θ are the azimuth and elevation angles, λ is the wavelength (5 mm at 60 GHz), and finally \top denotes transpose.

In our case, we consider URA antennas at both terminals having either 16 ($N_r=4$, $M_c=4$) or 64 ($N_r=8$, $M_c=8$) elements with Δl_r and Δl_c equal to 2λ . The channel matrix can be obtained by the matrix representation given by (3), where L is the number of propagation paths, β_i are the corresponding gains of each path arriving at the receive antenna, $\mathbf{A}(\phi_{R,i}, \theta_{R,i})$ and $\mathbf{A}(\phi_{T,i}, \theta_{T,i})$ are the array response and transmitter steering matrices respectively for the i -th path and H denotes conjugate transpose.

Hence, from (3) if we know the azimuth/elevation angle of arrival (AoA) and angle of departure (AoD) of each one of the L propagation

paths, the antenna elements and their spacing, we can calculate the channel matrix \mathbf{H} . The power gains β_i (complex received amplitude) of each path can be calculated using a multi-ray model that describes the signal propagation at the desired frequency. The reflected components may exhibit single, double or higher order reflection from a plane surface. The reflection geometry can be described in the horizontal as well as in the vertical plane. Hence, if we know the geometry of the environment where the signal propagates (length, width, height) and the surface reflection coefficients, the received amplitude of each reflected ray could be determined as well as the AoAs and AoDs of each ray. In our case we consider 13 reflected paths, given by (4), where d_0 is the path length of the direct component and d_i , d_j , d_k are the path lengths of the reflected rays. In addition, R_i is the reflection coefficient of i single reflected ray whereas R_{ja} , R_{jb} are the reflection coefficients of the j double reflected rays on a and b reflecting surfaces respectively and R_{ka} , R_{kb} , R_{kc} , are the reflection coefficients of the k triple reflected rays on a , b and c reflecting surfaces respectively. Moreover, $\Delta\phi_i = 2\pi\Delta l_i / \lambda$, $\Delta\phi_j = 2\pi\Delta l_j / \lambda$ and $\Delta\phi_k = 2\pi\Delta l_k / \lambda$ are the phase

differentials between the direct and the reflected rays with Δl_i , Δl_j and Δl_k the differential path lengths between the direct and the i single, j double and k reflected rays. Finally, after calculating the channel matrix \mathbf{H} , its capacity, assuming a channel unknown to the transmitter, can be easily obtained as a function of the signal to noise ratio (SNR), according to:

$$C = \log_2 \det \left(I + \frac{\rho}{n} \mathbf{H}\mathbf{H}^H \right) \quad (5)$$

where I is a unitary matrix, ρ is the SNR and n stands for the transmitter antenna elements. The capacity is referred as the error free spectral efficiency, or the data rate per unit bandwidth that can be sustained reliably over the MIMO link. Thus given a bandwidth B Hz, the maximum achievable data rate over this bandwidth using the MIMO channel will be $B \times C$ b/s.

3 Simulation Procedure

The studied environment is a corridor with dimensions $30 \text{ m} \times 1.75 \text{ m} \times 2.80 \text{ m}$. We assume $h_t=2 \text{ m}$ and $h_r=1.5 \text{ m}$, with the transmitter to be placed at the beginning of the corridor and 0.875 m from the right wall. The receiver moves along a straight line (0.5 m from the right wall), departs 1 m away from the transmitter and totally covers 25 m . The distance samples were $\lambda/4$ so as to calculate the received power and capacity along the corridor. The x-axis of propagation is considered to be along the corridor, whereas the URAs were placed at the y/z-plane at both terminals. The left and right wall surface is made of brick and plasterboard with wooden doors every 3 m but in order to simplify the simulation procedure we assume the surface as a uniform wall, made of brick and plasterboard with its dielectric characteristics given in Fig. 1.

The floor is made of concrete and covered with marble, whereas the suspended ceiling is made of aluminium sheets, holding the fluorescent light tubes. Furthermore, all the material characteristics are provided as well as the propagation geometry and the terminal positions. Each terminal it is assumed to have 16 or 64 elements orientated in the y/z plane as shown in Fig. 1.

In order to simplify the simulation procedure and reduce the calculation time, in (3), we use four single reflected, four double reflected four triple reflected rays, plus the direct component (13 reflected rays in total). Hence, \mathbf{H} will be a $(N_r \times M_c)$

$\times (N_r \times M_c)$ matrix, $\mathbf{A}(\phi_{R,i}, \theta_{R,i})$ a $(N_r \times M_c) \times 13$ matrix, and $\mathbf{A}(\phi_{T,i}, \theta_{T,i})$ a $(N_r \times M_c) \times 13$ matrix respectively. Some additional assumptions are:

- The diffraction is not taken into account since at 60 GHz the phenomenon is almost negligible and the diffracted power does not contribute to the total received power.
- The non-uniformities of the surface materials in indoor environments are such that the produced scattering has not a substantial contribution to the received power.
- The most significant contribution is from the 13 rays previously reported. Further reflected rays are not taken into account since their contribution to the total received power is insignificant.
- Up to third order reflections are taken into account, since fourth order reflections, especially at 60 GHz , are negligible contributors to the average power.
- Atmospheric propagation losses are not taken into account since in indoor environments the attenuation is very small (11.6 dB/km) [3].

During the entire simulation procedure vertical polarization is assumed. Hence, for the rays reflected from vertical walls we use the perpendicular reflection coefficient ($R_{s\perp}$), whereas for the rays from floor and ceiling surfaces we use the parallel reflection coefficient ($R_{s\parallel}$). Both reflection coefficients are given in [4]. In the reflection coefficient equations the complex dielectric constant [4] is given by $\epsilon = \epsilon_r - j60\sigma\lambda$ where ϵ_r is the relative dielectric constant of the reflecting surface, σ is the conductivity of the surface in Siemens/m and λ is the wavelength. The values of ϵ_r and σ are given in Fig. 1 [5], [6].

We considered three different antenna configurations; one element at both terminals (SISO system), 16 elements at both terminals (16×16 , MIMO system), and 64 elements at both terminal antennas (64×64 MIMO system). The simulation is conducted with Matlab script, using 13 rays in total. The channel matrix described by (3) was calculated for each predetermined scenario and for the three different antenna configurations. Then substituting the channel matrix \mathbf{H} in (5), the capacity of the channel in b/s/Hz was calculated as a function of the desired signal to noise ratio.

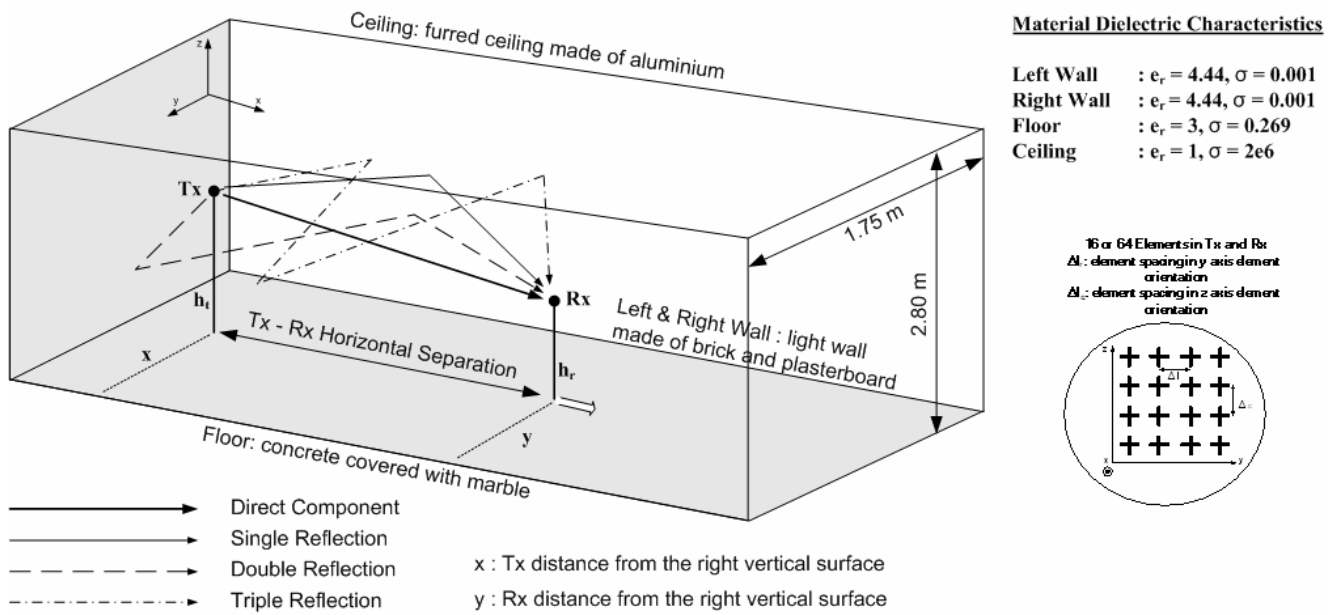


Fig. 1, Simulation environment, propagation geometry and material dielectric characteristics.

4 Simulation Results

An efficient system that operates with more than one element antennas is required to achieve a capacity greater than 1 b/s/Hz. Fig. 2(a) presents the received power as a function of distance along the corridor, predicted for three different antenna element configurations. It is evident that the multiple element configurations provide a fading improvement relatively to a SISO channel. For a 16x16 and 64x64 configuration, the fading is improved 10.2 and 18.4 dB respectively.

Taking into consideration the cumulative distribution function (CDF) of the calculated results, we may extract the distribution of the achieved channel capacity. Given a 10 dB SNR, from Fig. 2(b), we observe that the capacity decreases as the distance between the terminals increases taking steps of 5 m distance. In the 75% of the cases the capacity remains above 3 b/s/Hz for a MIMO 16x16 element configuration, as well as in the 90% of the cases the capacity remains above 4 b/s/Hz for a MIMO 64x64 element configuration, even when the receiver is 15 m away from the base station.

The channel capacities as a function of the SNR, for a 60 GHz system, derived by the aforementioned procedure, are illustrated in Fig. 2(c) and (d), whereas the distance between the transmitter and receiver has been selected 10 m. According to [1] the systems that operate at 60 GHz will be a part of fourth generation systems (4G) and may feature transmission rates up to 155 Mb/s especially in an indoor environment. In Europe two frequency segments having a bandwidth of 1 GHz have been allocated around 60 GHz. This will give the capability to allocate channels up to 100 MHz for

the users [7]. Hence, having a flat fading channel and 100 MHz bandwidth available and combining the results derived by the simulation procedure, we can achieve a transmission rate of 720 Mb/s for a 64x64 MIMO system with 10 dB SNR at a distance of 10 m from the transmitter, as we can see from Fig. 2(c). Achievable data rates can be more than 1 Gb/s provided that the SNR is doubled.

In [8], wideband channel measurements were performed in the same corridor, transmitting a bandwidth of 100 MHz. The results revealed that the channel exhibits frequency selective characteristics. The coherence bandwidth that determines the performance of a digital system was found 22.5 MHz for 90% correlation and 54 MHz for 75% correlation respectively. Accordingly, Fig. 3(d), presents the achieved data rate as a function of SNR in case a frequency selective channel (54 MHz bandwidth). As it is obvious very high data rates, even higher than 155 Mb/s, can be achieved maintaining low SNR, but in general lower rates than the flat fading channel. From both figures, the improvement from 16 to 64 element antenna selection has values from 110 up to 170 Mb/s for 54 MHz bandwidth and from 210 up to 250 Mb/s for 100 MHz bandwidth, in terms of the achieved channel data rate.

5 Conclusion

This paper presented a simulation procedure in an indoor environment at 60 GHz in order to evaluate the capacity by using multiple element antennas utilizing uniform rectangular array antennas.

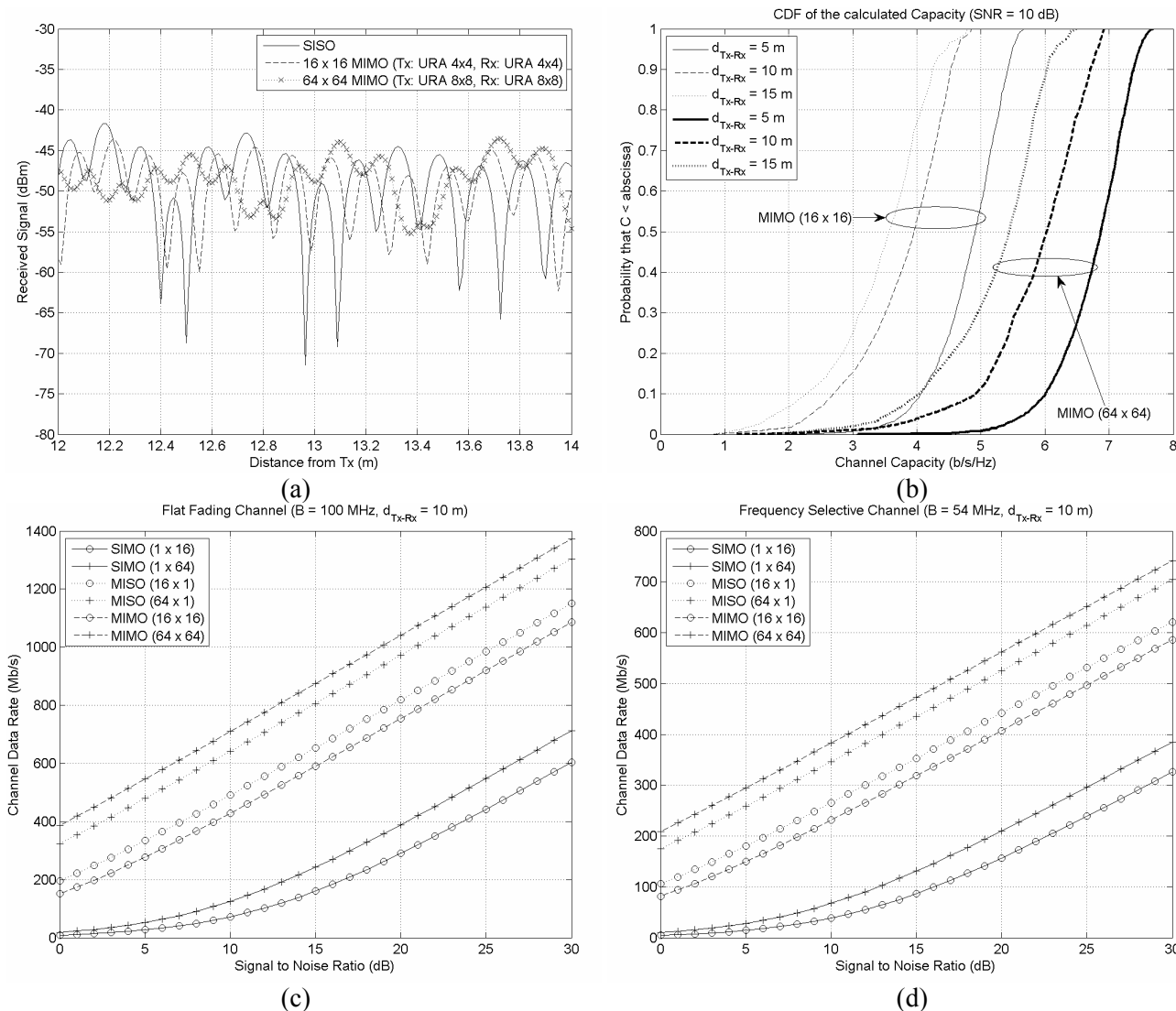


Fig. 2, Simulation results. (a) Received signal as a function of distance, (b) capacity CDF at various distances along the corridor, (c) channel data rate considering a flat fading channel, and (d) channel data rate in case of a frequency selective channel.

The channel model exploits the geometric characteristics of the environment, the AoA, AoD and the features of the antenna elements.

It was found, that the system capacity increases significantly if 16 or 64 MIMO elements are used at both terminal antennas instead of the basic SISO configuration. Furthermore, it was observed that in order to realize a major improvement in the data rates, a MIMO system at 60 GHz should operate at a distance up to 15 m with the view of maintaining low Signal to Noise Ratios yielding to a capacity of 4 b/s/Hz for the 90% of the cases. Efficient data rates up to 1 Gb/s for a 64x64 MIMO systems can be obtained relative to a SIMO or MISO system, while the volume of SNR is equal and over 10 dB.

References:

[1] P. Smulders, "Exploiting the 60 GHz band for local wireless multimedia access: prospects and

future directions," IEEE Commun. Mag., vol. 40, no. 1, pp. 140-147, Jan. 2002.

- [2] A. Paulraj, R. Nabar, and D. Gore, Introduction to space-time wireless communications, Cambridge University Press, 2003.
- [3] N. Moraitis, and P. Constantinou, "Indoor channel measurements and characterization at 60 GHz for wireless local area network applications," IEEE Trans. Antennas Propagat., vol. 52, no. 12, pp. 3180-3189, Dec. 2004.
- [4] T. S. Rappaport, Wireless Communications, Upper Saddle River, NJ: Prentice Hall, 1996.
- [5] K. Sato et al, "Measurements of the complex refractive index of concrete at 57.5 GHz," IEEE Trans. Antennas Propagat., vol. 44, no. 1, pp. 35-39, Jan. 1996.
- [6] K. Sato et al., "Measurements of reflection and transmission characteristics of interior structures of office building in the 60-GHz

band,” IEEE Trans. Antennas Propagat., vol. 45, no. 12, pp. 1783-1792, Dec. 1997.

- [7] R. Prasad, “Overview of wireless communications: Microwave perspectives”, IEEE Commun. Mag., pp. 104-108, Apr. 1997.
- [8] N. Moraitis, and P. Constantinou, “Millimeter wave propagation measurements and characterization in an indoor environment for wireless 4G systems, in Proc. PIMRC '05, Sep. 2005.